5.4 References

Aas, W., Hjellbrekke, A.-G., and Schaug, J., 2000, Data quality 1998, quality assurance and field comparisons, Norwegian Institute for Air Research, EMEP/CCC Report 6/2000.

Mylona, S., 1999, EMEP emission data: Status report 1999, EMEP/MSC-W Note 1/99, The Norwegian Meteorological Institute, Oslo, Norway.

Roemer, M., Dreiem, R., Hanssen, J. E., and Tørseth, K., 1998, Evaluation of ozone measurement data at the sites Birkenes, Jeløya and Prestebakke over the period 1988-1995, Norwegian Institute for Air Research, NILU TR 2/98.

Simpson, D., Olendrzyński, K., Semb, A., Støren, E., and Unger, S., 1997, Photochemical oxidant modelling in Europe: multi-annual modelling and source-receptor relationships, Norwegian Meteorological Institute, EMEP MSC-W Report 3/97.

Chapter 6

On the Distribution of Sea Salt and Sodium Nitrate Particles in Europe.

Jan E. Jonson, Arne Semb, Kevin Barrett, Alf Grini and Svetlana Tsyro

6.1 Introduction:

Up to now particulate nitrate has been represented in the Eulerian models as ammonium nitrate only. Over the oceans, where very little ammonia is available, total nitrate has mostly been in the form of HNO_3. Comparisons with measurements has revealed that the model in general underestimates the total nitrate concentrations at Scandinavian sites, and furthermore that this underestimation increase farther away from the major source areas. As the dry deposition of HNO_3 is faster than for particulate nitrate, this could be explained by the low fraction of total nitrate in the form of particles. A parameterisation of sea salt particles and sodium nitrate is therefore tested. The parameterization, and the effects on the calculations are described in this chapter.

6.1.1 Sea salt and sodium nitrate particles.

Both sea salt and sodium nitrate particles are included in the model using a bulk parameterization (the particles are treated as if they all have the same size). The mean particle diameter with respect to mass is assumed to be 6μm and 3.2μm for sea salt and sodium nitrate particles respectively.

Sea salt production.

The production of sea salt particles is parameterized as a function of wind speed only. The relationship between wind speed and sea salt production is similar to the expression used by Pryor and Sørensen (1999), but for a bulk formulation. We have not included the production from spume at high wind speeds.

$$P_{ssalt} = U_{10}^{3.41} \times 0.007 \tag{6.1}$$

where P_{ssalt} is in g m^{-2} s^{-1}, and U_{10} is the wind speed at 10 m height (m s^{-1}), calculated from the surface wind stress assuming a logarithmic wind profile.

Sea salt - nitric acid interactions.

The interaction between sea salt and HNO_3 may be viewed as three separate processes.

1. Mass transfer of gaseous HNO_3 to the sea salt aerosol surface.
2. Chemical reaction on the aerosol surface between HNO_3 and NaCl.

3. Driving off HCl from the aerosol to the gas phase.

The rate constant for the reaction between HNO_3 and NaCl is known to be fast (Fenter et al., 1994). We assume that the first process is the rate limiting step.

Assuming a log-normal size distribution for the sea salt aerosols with a mean droplet radius of 1.66μm, corresponding to the sea salt aerosol with the largest surface area with a standard deviation of ln 0.191, Sander and Crutzen (1996) calculates the mean transfer coefficients for a number of components. For HNO_3 the calculated mean transfer coefficient k_t is 2.8×10^6 s^{-1}. Assuming zero concentration of HNO_3 on the aerosol surface the loss rate of HNO_3 to the sea salt aerosols is calculated as: $Q = k_t \times L$, where L is the volume ratio of sea salt aerosols to air. L is calculated from the sea salt concentration assuming a volume ratio of 1:10 for NaCl and liquid water in the aerosols. With a sea salt concentration of 10μg m^{-3} we then calculate a characteristic lifetime for HNO_3 in the boundary layer against aerosol uptake of the order of 1 hour.

Dry deposition.

The dry deposition of particles is strongly dependent on particle size and wind speed, spanning orders of magnitude. The dry-deposition parameterization scheme applied for sea salt and sodium nitrate particles is based on the parameterization from Seinfeld and Pandis (1998). This formulation use the resistance analogy where the dry deposition at 1m for monodisperse particles, v_{dm}, are calculated according to the equation

$$v_{dm} = \frac{1}{r_b + r_b v_g} + v_g \tag{6.2}$$

where r_b is the quasi laminar resistance and v_g is gravitational settling velocity of the particles. With a monodisperse size distribution the dry deposition is likely to be underestimated. To correct for this effect the mass averaged dry deposition at 1m is scaled as suggested by Slinn and Slinn (1980)

$$v_d = v_{dm} \times \exp\left(2(ln\sigma_g)^2\right) \tag{6.3}$$

where σ_g is the standard deviation for the size distribution. In the calculations we have used a standard deviation of 2 for the size distribution.

The aerodynamic resistance is calculated as in previous versions of the EMEP Eulerian Acid deposition model (Berge and Jakobsen, 1998, Jonson et al., 1998). An effective dry deposition velocity for the lowest model layer, v_h, is calculated from the equation:

$$v_h = \frac{v_d}{1 + \frac{v_d}{C_H|\vec{V_H}|}} \tag{6.4}$$

where V_H is the horizontal wind vector, C_H is the drag coefficient and v_d the dry deposition velocity at 1 m. The drag coefficient is calculated from Monin Obukhov similarity theory as described by Berge and Jakobsen (1998).

6.1.2 Sea salt and sodium nitrate: Model results.

As seen in Figure 6.3 , sea salt is mainly confined to the oceans where monthly averaged concentrations range from 10 to 15μgm^{-3} in January and 5 to 10μgm^{-3} in July. $NaNO_3$ typically accounts for more than 80% of the total nitrate over the ocean throughout the year (Figure 6.4). Over the European continent typically less than 20% of the calculated total nitrate is in the form of $NaNO_3$ in January, but, unexpectedly, in summer the fraction is much higher than in winter. The low fraction in winter can be explained by a "continental winter" with easterly winds in 1996. In Figure 6.1 and 6.2 calculated sea salt concentrations are compared to measurements at several sites in Norway. Apart from for Birkenes and Skreådalen, calculated sea salt levels compare reasonable well with observation. For sea salt, with such a short lifetime in the atmosphere, a significant improvement in the calculated results will require a better model resolution.

Figure 6.5 depicts the sodium nitrate concentration as calculated by the model. High levels are mainly confined to sea areas close to the European mainland. In particular in January, with easterly winds dominating, the gradient between land and sea is very clear.

Table 6.1: Annual means and correlations between model and measurements for total nitrate as $\mu g(N)m^{-3}$ at the individual measurement sites. Calc 1. and corr. 1 refers to the calculations with $NaNO_3$, Calc 2. and corr. 2 to the calculations without $NaNO_3$

Site	Obs.mean	Calc. mean 1	Corr. 1	Calc. mean 2	Corr. 2
Skreådalen	0.251	0.293	0.791	0.289	0.817
Birkenes	0.286	0.321	0.656	0.276	0.661
Osen	0.136	0.114	0.614	0.100	0.583
Kårvatn	0.084	0.044	0.495	0.039	0.515
Tustervatn	0.105	0.033	0.268	0.028	0.477
Jergul	0.084	0.026	-0.072	0.021	0.287

In Table 6.1.2 and in Figures 6.6 and 6.7 calculated concentrations of total nitrate (with and without the inclusion of sodium nitrate) are compared to measurements for some Norwegian sites. The inclusion of $NaNO_3$ in the model leads to an increase in calculated total nitrate at all locations showed. However, total nitrate is still under-predicted at long distances from major source areas also after the introduction of $NaNO_3$ in the model. The correlation between calculated and measured concentrations decrease after the inclusion of sodium nitrate. Sodium nitrate may also be formed from NO_2, via N_2O_5, on the seasalt particles (Hara et al., 1999), providing an extra source for total nitrate not included in the model. This is unlikely to be a major source of sodium nitrate, and other explanations for the deficit of total nitrate at remote locations should be sought.

6.2 References

Berge, E. and Jakobsen, H. A., 1998, A regional scale multi-layer model for the calculation of long-term transport and deposition of air pollution in Europe, *Tellus*, 50, 205–223.

Fenter, F.F., Calos, F., and Rossi, M.J., 1994, Kinetics of nitric acid uptake by salt, *J. Phys. Chem.*, 98, 9801–9810.

Hara, K., Osada, K., Hayashi, M., Matsunaga, K., Shibata, T., and Iwasakaet, Y., 1999, Fractionation of inorganic nitrates in winter arctic troposphere: Coarce aerosol particles containing inorganic nitrates, *J. Geophys. Res.*, 104, 23,671–23,679.

Jonson, J. E., Tarrason, L , and Sundet, J.K., 1998, The Eulerian 3-D oxidant model: Status and evaluation for summer 1996 results and case-studies, In *Transboundary photo-oxidant air pollution in Europe.* EMEP/MSC-W Status Report 2/98, The Norwegian Meteorological Institute, Oslo, Norway.

Pryor, S.C. and Sørensen, L.L., 1999, Nitric acid - sea salt reactions: implications for nitrogen deposition to water surfaces, *J. of Applied Meteorology*, Submitted.

Sander, Rolf and Crutzen, Paul J., 1996, Model study indicating halogen activation and ozone destruction in polluted air masses transported to the sea, *J. Geophys. Res.*, 101, 9121–9138.

Seinfeld, J.H. and Pandis, S.N., 1998, *Atmospheric chemistry and physics. From air pollution to climate change* , John Wiley and Sons, inc., New York.

Slinn, S. A. and Slinn, W. G. N., 1980, Predictions for particle deposition on natural waters, *Atmos. Environ.*, 14, 1,013–1,016.

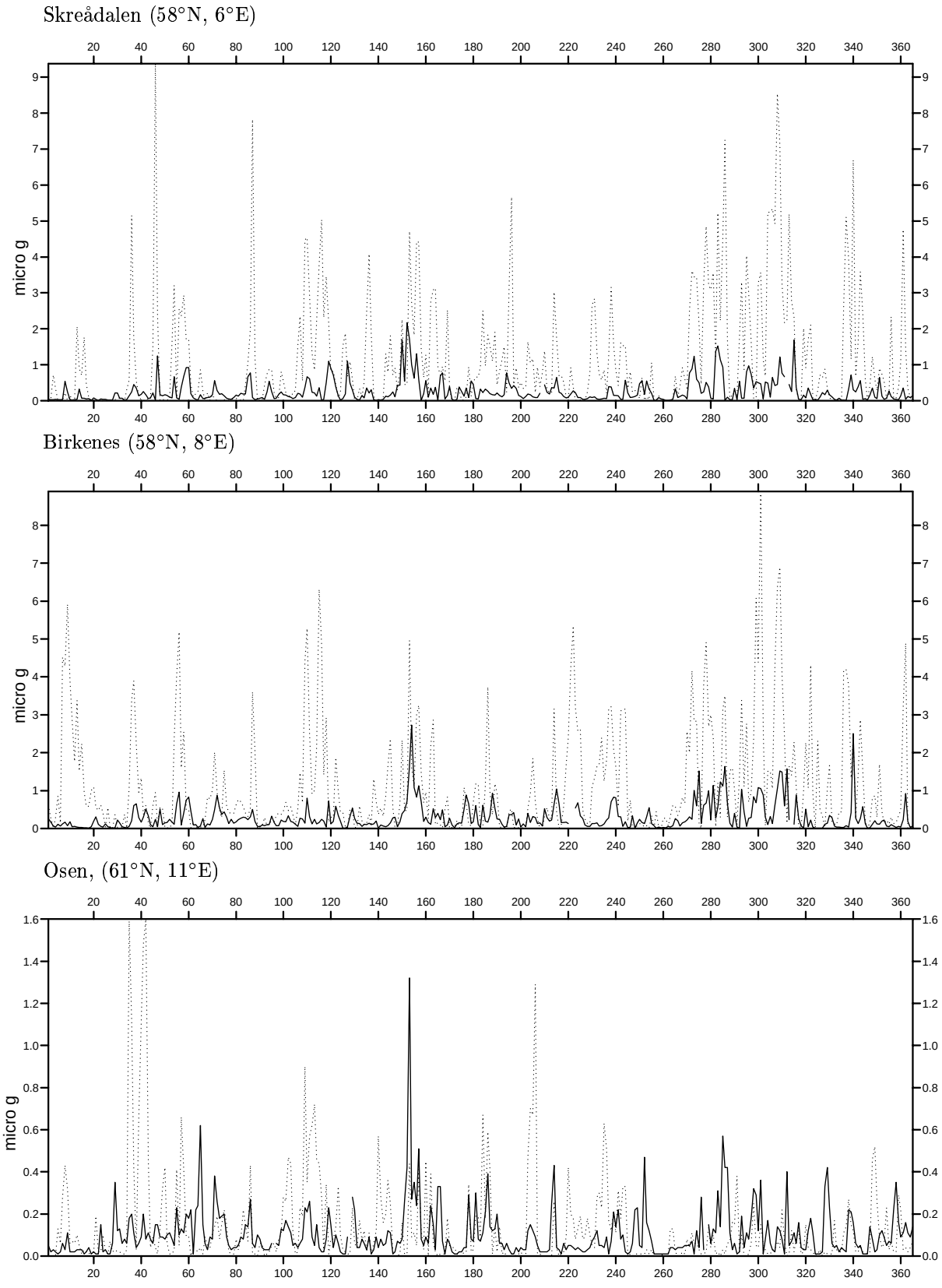

Figure 6.1: Measured (full line) versus calculated (dotted line) daily averaged concentrations of seasalt in μg(Na)cm^{-3}, calculations for 1996.

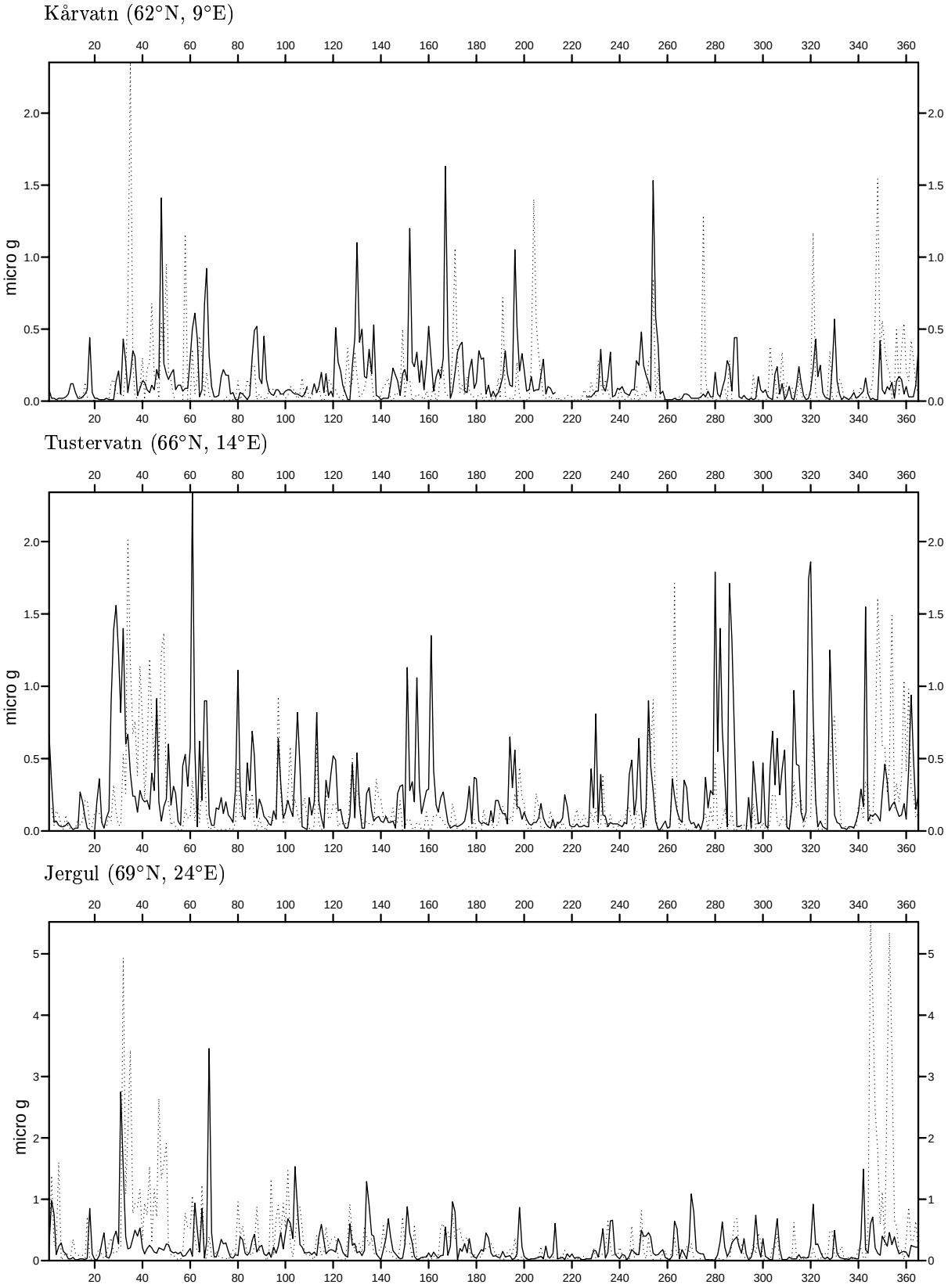

Figure 6.2: Measured (full line) versus calculated (dotted line) daily averaged concentrations of seasalt inμg(Na)cm^{-3}, calculations for 1996.